0026-895X/96/061612-07$3.00/0

MOLECULAR PHARMACOLOGY, 50:1612–1618 (1996).

Acid-Catalyzed Oxidation of the Anticancer Agent Mitoxantrone by Nitrite Ions

KRZYSZTOF J. RESZKA and COLIN F. CHIGNELL

Laboratory of Molecular Biophysics, National Institute of Environmental Health Sciences, National Institutes of Health, Research Triangle Park, North Carolina 27709

Received April 29, 1996; Accepted August 26, 1996

SUMMARY

Mitoxantrone (1,4-dihydroxy-5,8-bis{2-[(2-hydroxyethyl)amino-]ethyl}amino-9,10-anthracenedione; MXH_2) is a novel anticancer agent that is useful in the treatment of leukemia and breast cancer. In contrast to other anthracenedione-based agents, this drug causes fewer side effects, mainly because it is resistant to metabolic reduction. We investigated the interaction between MXH_2 and inorganic nitrite (NO_2^-) in aqueous solutions and found that this drug undergoes acid-catalyzed oxidation by nitrite. The rate of this reaction measured versus [$NaNO_2$] at constant pH or versus pH at constant [$NaNO_2$] was found to be directly proportional to the actual HNO_2 concentration, indicating HNO_2 to be the major oxidizing species. Involvement of $^{\cdot}NO$ and/or $NO_2^{\cdot}$ radicals as minor oxidants is suggested based on the dependence of the rate of oxidation on the presence of air. Spectrophotometric and electron paramagnetic resonance analyses indicate that early products of the reaction are identical to those generated by oxidation of MXH_2 by a horseradish peroxidase/hydrogen peroxide system. The major product is hexahydronaphtho[2,3-*f*]quinoxaline-7,12-dione, which is formed by intramolecular cyclization of one alkylamino side chain in the oxidized, diiminoquinone MX(N) form of the drug. This study shows that MXH_2 effectively scavenges HNO_2 and possibly other nitrogen oxides. Because these reactive forms of nitrogen may be present *in vivo*, this property of the drug may be relevant to its biological or perhaps anticancer activities.

MXH_2 (1,4-dihydroxy-5,8-bis{2-[(2-hydroxyethyl)amino]-ethyl}amino-9,10-anthracenedione) (Fig. 1) is a novel anthracenedione-based anticancer agent that is effective against certain types of malignancies, especially leukemia and breast cancer (1, 2). The drug shows markedly diminished cardiotoxicity compared with that of the more widely used anticancer agents adriamycin and daunorubicin (2–5) while still retaining anticancer activity. It is therefore an attractive alternative drug in cancer chemotherapy.

The exact mechanism of action of MXH_2 is unknown, although it has been linked to the ability of the drug to bind to DNA (6) and to inhibit DNA and RNA synthesis (7). In contrast to other quinone-based anticancer agents, MXH_2 does not readily undergo metabolic reduction and does not redox cycle (8, 9). Recent evidence shows that the biological activity of the drug may be due to oxidative activation. It has been reported that HRP/H_2O_2, cytochrome P450, and myeloperoxidase/H_2O_2 oxidize MXH_2 (10–14) to a metabolite, which has been identified as MH_2 (hexahydronaphtho[2,3-*f*]quinoxaline-7,12-dione) (Fig. 1), formed by intramolecular nucleophilic addition of the side-chain amino group to the ring C7 atom (12). This structural transformation of the drug chromophore renders its oxidation an irreversible process.

The major metabolite MH_2 is a redox active compound. It can be readily oxidized by HRP/H_2O_2 and then reduced to MH_2 by good electron donors such as ascorbate (11). Thus, it seems that the oxidative transformation of MXH_2 contains irreversible as well as reversible steps, as described by eq. 1.

$$MXH_2 \xrightarrow{-2e} MXH_2^{2+}\ (\text{oxidized}) \underset{\text{X}}{\overset{\text{cyclization}}{\rightleftharpoons}} MH_2 \overset{-2e}{\underset{+2e}{\rightleftharpoons}} MH_2^{2+} \quad (1)$$

We studied the reactions of MXH_2 in the presence of NO_2^- as a function of pH and found that in acidic solutions the drug undergoes oxidation. HNO_2 has been identified as the most important oxidizing species. The rationale behind this study is that (i) MXH_2 is administered intravenously to cancer patients (2) and therefore it may interact directly with blood components. (ii) The pH of many cancer cells is acidic. Although the pH values in various malignant tumors are in the range of 6.0–6.5 (15), values as low as 4 and 3 were reported for solid tumors (16). (iii) In this acidic environment, NO_2^- exist partially as HNO_2 [pK_a (HNO_2/NO_2^-) = 3.35] (17). The primary source of nitrite *in vivo* is the diet. Another source of the nitrite may be aerobic oxidation of $^{\cdot}NO$ (18). $^{\cdot}NO$ is produced metabolically by various types of cells and by activated macrophages and neutrophils in the blood (18, 19). (iv) HNO_2 is a potent oxidant known to react with phenols, hydroquinones, and aromatic amines (20–22). These functional

ABBREVIATIONS: HRP, horseradish peroxidase; EPR, electron paramagnetic resonance; MXH_2, mitoxantrone.

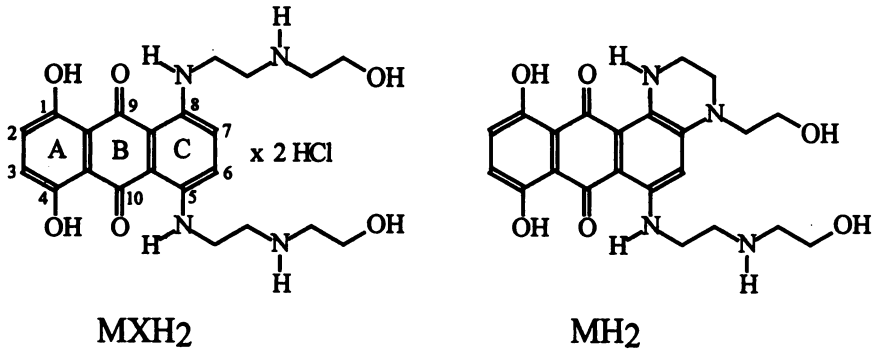

Fig. 1. Structures of MXH_2 and its cyclized oxidation product, MH_2.

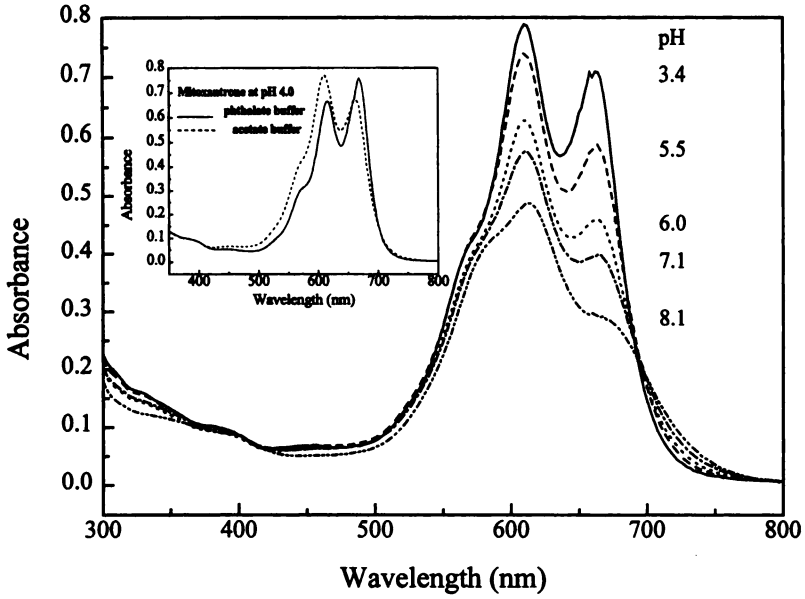

Fig. 2. Absorption spectra of MXH_2 (0.1 mM) measured at pH 3.4 (*unbroken*), 5.5 (*dashes*), 6.0 (*dots*), 7.1 (*dash/dot*), and 8.1 (*dash/dot/dot*). (UV cell light path, 0.4 cm). *Inset*, absorption spectra of MXH_2 at pH 4.0 in phthalate and acetate buffers (0.1 M).

groups are present in the MXH_2 structure (Fig. 1). It is therefore likely that reactions of MXH_2 with HNO_2 that we describe could model some intracellular processes of the drug *in vivo*.

Materials and Methods

MXH_2 (the dihydrochloride form) was obtained from the Drug Synthesis and Chemistry Branch, Developmental Therapeutic Program, Division of Cancer Treatment, National Cancer Institute (Bethesda, MD). Sodium nitrite (99.9%) and HRP (Type VI) were from Sigma Chemical (St. Louis, MO). H_2O_2 (30%; Fisher Scientific, Fair Lawn, NJ) was diluted, and its concentration was determined spectrophotometrically at 240 nm using molar absorptivity of 39.4 M^{-1} cm^{-1}. Stock solutions of MXH_2 (11 mM) and nitrite (1 M) were prepared in deionized water. Measurements were performed in acetate and phthalate buffers (0.1 M) for the pH 3.4–6.0, and in phosphate buffers (0.05 M) for pH 7.1 and 8.1. Absorption spectra were measured in a quartz cuvette (0.4-cm light path) using Hewlett-Packard diode array spectrophotometer model 8451A (Palo Alto, CA).

Kinetic measurements were carried out by measuring the time course of the absorbance at 662 nm corresponding to the absorption maximum of the monomeric form of the drug. The rates of the oxidation of MXH_2 were calculated directly from the experimental kinetic runs (see Fig. 5A). Because the kinetic runs began at different levels depending on pH, the rates were also calculated taking into account differences in the initial concentrations of monomers. This was accomplished by deconvoluting the experimental absorption spectra of MXH_2, obtained at pH 3.4–6.0, in the 450–750-nm range using Microcal Origin (version 3.5; Northampton, MA). The best fits were obtained using four gaussian curves,[1] and the peak heights at 662 nm were normalized to that at pH 3.4 (100% monomer). Rates calculated using these two approaches gave identical results.

EPR measurements were carried out using a Varian E-109 Century Line EPR spectrometer (Palo Alto, CA) operating at 9.5 GHz with 100 kHz modulation. Samples were transferred to an aqueous flat quartz EPR cell, and the first scan was started <1 min after the start of the reaction (i.e., the addition of nitrite). Subsequent scans were executed at defined time intervals. Values for g factors of the MXH_2-derived radicals were determined versus a standard (Fremy's salt, g = 2.0055) in a capillary attached to the EPR cell.

Results

Absorption Spectra

The UV/VIS absorption spectra of MXH_2 measured in solutions of varying pH are shown in Fig. 2. The compound has two absorption maxima in the visible region, at 662 nm and 612 nm, and a shoulder around 570 nm. The optical properties of the drug are concentration and pH dependent (23, 24); this is because the drug molecules show a strong propensity to form dimers especially at or near neutral pH. With more acidic solutions, the absorption maximum at 662 nm increases (Fig. 2), which corresponds to an increase in the concentration of the monomeric form of the drug. Spectral

[1] The curves were centered at 662, 610, and 569 nm. The λ_{max} of the fourth peak was pH dependent, ranging from 537 to 553 nm.

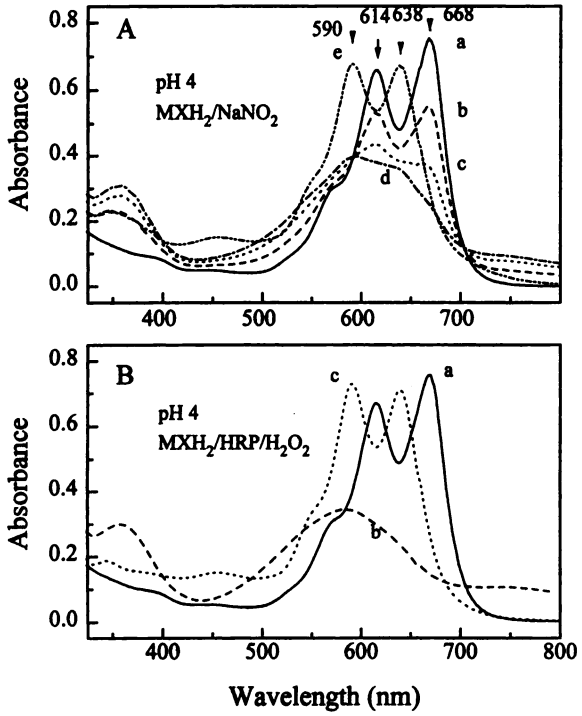

Fig. 3. Absorption spectra of MXH_2 (0.1 mM) at pH 4.0 (aerated phthalate buffer, 0.1 M). A, In the presence of $NaNO_2$ (5 mM). *a*, Before $NaNO_2$ addition. *b–d*, Recorded at 1-min intervals. *e*, Observed after sodium ascorbate addition (excess) to sample *d*. B, Spectra observed during oxidation of MXH_2 (0.1 mM) by HRP/H_2O_2; [HRP] = 10 μg/ml, $[H_2O_2]$ = 1.5 mM. *a*, MXH_2 and H_2O_2 before HRP addition. *b*, After HRP addition. *c*, After ascorbate (excess) addition to sample *b*.

lines measured in acetate buffers at pH 3.4–6.0 show an isosbestic point at λ_{iso} = 682 nm (Fig. 2), confirming that in this pH range MXH_2 exists predominantly in monomeric and dimeric forms. We noticed that in phthalate buffers, the concentrations of monomers tended to be higher compared with those in acetate buffers at the same pH (Fig. 2, *inset*). Nevertheless, reactions of the drug with nitrite in acetate and phthalate buffers occurred with similar rates and afforded identical products.[2]

Interaction of MXH_2 with NO_2^-

The reaction of MXH_2 with nitrite was studied by measuring the absorption spectrum of the drug as a function of pH, nitrite concentration, and time of reaction. EPR experiments were carried out to determine whether the reaction of MXH_2 with nitrite gives rise to free radical products. The results were compared with those from parallel experiments, in which the drug was oxidized by HRP/H_2O_2 under otherwise identical conditions.

Spectrophotometric study. The addition of $NaNO_2$ to MXH_2 in acidic buffers caused the absorption maxima of MXH_2 at 612 and 662 nm to decrease. Simultaneously, the color of the solutions turned from blue to magenta. Fig. 3A shows the corresponding absorption spectra recorded during successive intervals at pH 4.0 (phthalate buffer). These spectral changes indicate that the drug undergoes oxidation because similar behavior was observed when MXH_2 was treated with an enzymatic oxidation system, HRP/H_2O_2, at pH 4.0 (Fig. 3B). When ascorbate, a reducing agent, was added to the MXH_2 solution treated with nitrite, strong new absorption bands developed, with λ_{max} at 590 and 638 nm (Fig. 3A, *e*). A similar spectrum was observed when ascorbate was added to the sample containing MXH_2 oxidized with HRP/H_2O_2 (Fig. 3B, *c*). Therefore, the ascorbate-generated absorption spectra in Fig. 3, A and B, are assigned to MH_2, the reduced form of the MXH_2 oxidation product (11, 12).

Fig. 4 shows spectra of MXH_2 in acetate buffer, pH 5.5, recorded before and after the addition of nitrite and HRP/H_2O_2. In general, the oxidation of MXH_2 in acetic and phthalate buffers proceeded in a similar manner, with the major difference being that in the former buffers the spectra of the reduced product, MH_2 (Fig. 4A, *d*; Fig. 4B, *e*), have only one well-developed maximum at 588 nm and a shoulder at 636 nm. This is in contrast to the spectra in phthalate buffers, which showed two maxima (Fig. 3). Thus, it seems that in acetate buffers, molecules of the newly formed MH_2 chromophore are extensively dimerized. These observations are in agreement with earlier reports on MXH_2 oxidation by HRP/H_2O_2 (11, 12).

We note that after the reaction with ascorbate, the intensities of the bands at 588 nm at pH 5.5 in the $MXH_2/NaNO_2$ and $MXH_2/HRP/H_2O_2$ systems (Fig. 4, A and B) were very similar, suggesting that in both samples the amounts of accumulated oxidation products were almost the same. The same pattern was observed at pH 4.0 (Fig. 3, A and B). From

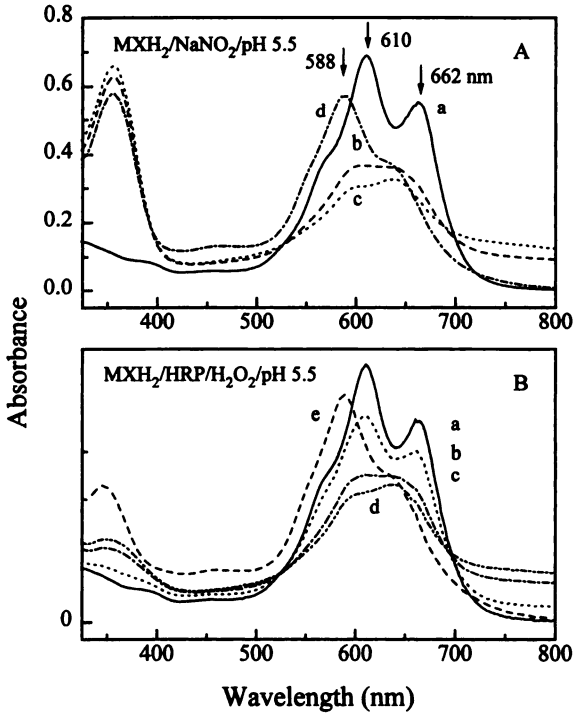

Fig. 4. Absorption spectra observed during oxidation of MXH_2 (0.1 mM) at pH 5.5 (aerated acetate buffer, 0.1 M) using (A) $NaNO_2$ and (B) HRP/H_2O_2. *a*, Before oxidation. A, *b* and *c*, Recorded 1 and 2 min after nitrite addition. $[NaNO_2]$ = 46.7 mM B, *b–d*, Recorded 60, 120, and 150 sec after initiation of the reaction with HRP. [HRP] = 2.5 μg/ml; $[H_2O_2]$ = 210 μM. Spectra *d* (A) and *e* (B) were observed after the addition of an excess of ascorbate to the oxidized MXH_2 solutions.

[2] Absorption spectra produced by treating MXH_2 with HNO_2 in acetate and phthalate buffers of the same pH showed some differences. Similar differences were observed when MXH_2 was oxidized by HRP/H_2O_2 in these buffers. However, the spectra of MXH_2 reacting with HNO_2 and with HRP/H_2O_2 in phthalate buffer are identical. Also, the spectra from MXH_2/HNO_2 and $MXH_2/HRP/H_2O_2$ in acetate buffer are similar.

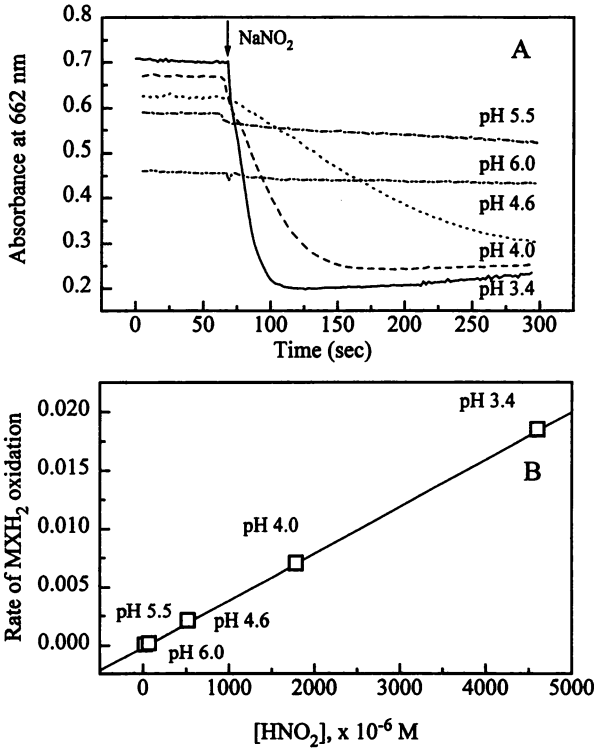

Fig. 5. Effect of pH on the oxidation of MXH_2. A, Time course of the absorbance at 662 nm of MXH_2 recorded at varying pH; [$NaNO_2$] = constant (9.8 mM). B, Dependence of the rate of MXH_2 oxidation on the HNO_2 concentration. Oxidation of MXH_2 (0.1 mM) was followed by measurement of the decrease in absorbance at 662 nm. *Arrow*, time of the addition of nitrite (10 μl of 1 M $NaNO_2$). The [HNO_2] concentration was calculated using the formula: $[HNO_2] = [H^+][T]/(K + [H^+])$, where ([T] = [$HNO_2$] + [$NO_2^-$]) is total nitrite concentration (9.8 mM), and K is the HNO_2 ionization constant [pK_a (HNO_2/NO_2^-) = 3.35].

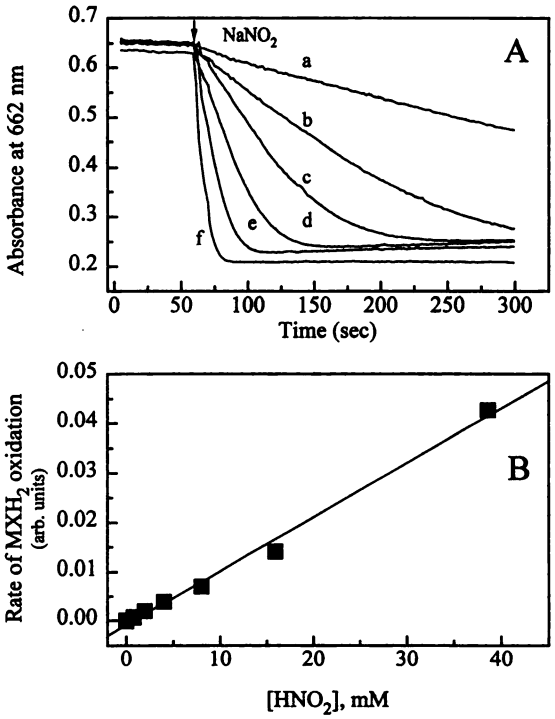

Fig. 6. Oxidation of MXH_2 (0.1 mM) by nitrite at pH 4.0 measured as decrease of the drug absorbance at 662 nm. A, Kinetic runs *a–f* were recorded at [$NaNO_2$] of 0.98, 2.4, 4.9, 9.8, 19.4, and 47.2 mM ([HNO_2] = 0.8, 1.96, 4.0, 8.0, 15.9, and 38.6, respectively). *Arrow*, time of the addition of $NaNO_2$. B, Dependence of the rate of MXH_2 oxidation on [HNO_2] at constant pH 4.0.

this we infer that the major reaction pathway in the presence of nitrite is MXH_2 oxidation and that other reaction routes, such as nitration or nitrosation of the drug molecules, are less important (*vide infra*).

The kinetics of drug oxidation was measured by following the decay of the absorption at 662 nm at varying pH values; we found that the rates increase sharply as the acidity of the solution increases (Fig. 5A). Because in acidic solutions NO_2^- may partially exist as HNO_2 (eq. 2) [pK_a (HNO_2/NO_2^-) = 3.35 (17)], this observation suggested that

$$NO_2^- + H^+ \rightleftarrows HNO_2 \qquad (2)$$

HNO_2 may be involved in MXH_2 oxidation. To verify this hypothesis, we determined the rates of MXH_2 oxidation at different pH values and related them to HNO_2 concentration at the respective pH values.[3] The concentrations of HNO_2 were calculated using the known concentrations of NO_2^- (added in the form of $NaNO_2$), the actual pH of the buffer, and the acid pK_a *value of 3.35. When the initial rates of* MXH_2 oxidation were plotted versus the HNO_2 concentrations calculated for a given pH value at constant [$NaNO_2$], a linear relationship was obtained (Fig. 5B), consistent with the hypothesis that HNO_2 is involved.

Fig. 6 shows the kinetics of MXH_2 oxidation recorded at a constant pH of 4.0 but at various $NaNO_2$ concentrations. The rates of oxidation, determined from the kinetic runs in Fig. 6A, are linearly dependent on [HNO_2] (Fig. 6B). This further confirms that HNO_2 is involved in MXH_2 oxidation.

The rate of drug oxidation depends on the presence of oxygen and is lower in nitrogen-saturated buffer than in air-saturated samples. For example, in a system containing MXH_2 (0.05 mM) AND $NaNO_2$ (24 mM), the absorption at 668 nm decreased by ~78% in 80 sec in an air-saturated pH 4.0 buffer (phthalate) versus 54% in a N_2-purged buffer. This suggests that in addition to HNO_2, other transients derived from HNO_2 may be involved in the drug oxidation. Possible candidates are $NO_2^{\cdot}$ and $^{\cdot}NO$ radicals, which can be formed according to eqs. 3 and 4. In aerated solutions, the concentration of the strongly oxidizing $NO_2^{\cdot}$ species may be higher than that in air-free samples, on the basis of eq. 5.

$$2\,HNO_2 \rightleftarrows N_2O_3 + H_2O \qquad (3)$$

$$N_2O_3 \rightleftarrows {}^{\cdot}NO + NO_2^{\cdot} \qquad (4)$$

$$2\,{}^{\cdot}NO + O_2 \rightarrow 2\,NO_2^{\cdot} \qquad (5)$$

NO_2 radicals have been shown to oxidize phenols and hydroquinones and to react with aromatic amines (25–27). Also, nitric oxide has the potential to produce radicals from phenolic compounds (28, 29). It is therefore likely that MXH_2 is oxidized not only by HNO_2 but also, although to a smaller

[3] Because the content of the monomers and the corresponding absorbance at 662 nm increase as the acidity in solutions increases, the kinetic runs measured in buffers of different pH started from different levels (Fig. 5A). These differences in the initial concentration of monomers were taken into account when calculating rates of the oxidation of MXH_2 as described in Materials and Methods.

extent, by $NO_2^{\cdot}$ and possibly $^{\cdot}NO$ radicals. This aspect of the MXH_2 chemistry is under investigation.

EPR measurements. It has been reported that oxidation of MXH_2 by HRP/H_2O_2 generates drug-derived radicals as demonstrated by the detection of an EPR signal (11). We found that the interaction of MXH_2 with nitrite in acidic solutions also leads to free radical products. Fig. 7A shows EPR signals recorded in intervals from a sample containing MXH_2 (1 mM) and sodium nitrite (10 mM) at pH 3.9. The amplitude of this signal gradually increased over a period of several minutes and then started to decrease. The line width of this signal was ~12.5 G, and its g value was determined to be 2.0032. Change in modulation amplitude or microwave power had no effect on the resolution of the spectra.

The EPR signal observed during oxidation of MXH_2 by HRP/H_2O_2 at pH 3.9 is shown in Fig. 7B. Its g value was 2.0032, and its line width was ~11.7 G. Thus, the two signals are very similar. This suggests that radicals produced by these two oxidizing systems are also similar or perhaps even identical, at least during the early stages of the reaction. This seems reasonable because HNO_2, $NO_2^{\cdot}$, and HRP/H_2O_2 function as one-electron oxidants, and therefore oxidation of MXH_2 by these systems could result in the formation of the same radicals. Prolonged reaction of MXH_2 with HNO_2 may, however, yield nitrosated products (*vide infra*), which may then give rise to different radical species. It is likely that the small difference in line widths of the EPR signals produced through oxidation of the drug by nitrite and by HRP/H_2O_2 (Fig. 7) may have this origin.

Discussion

We studied reactions between MXH_2 and nitrite anion in acidic solutions and found that the drug undergoes acid-catalyzed oxidation by nitrite, with HNO_2 as the most important oxidizing species. This conclusion is supported by the excellent correlation between the rate of MXH_2 oxidation and the HNO_2 concentration (Figs. 5 and 6).

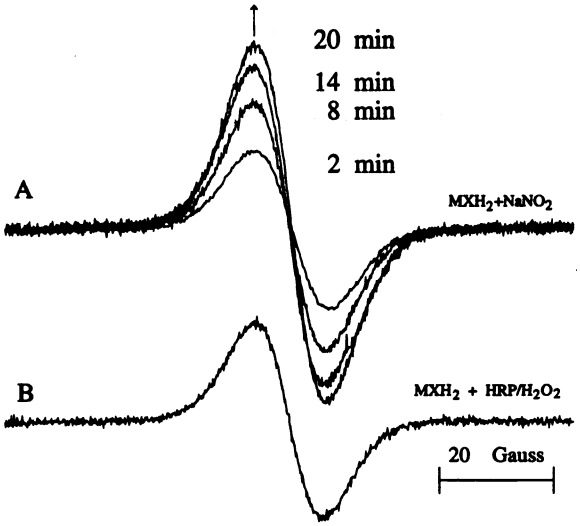

Fig. 7. EPR spectra of MXH_2-derived radicals generated by oxidation of the drug at pH 3.9 by (A) nitrite (A) and (B) an HRP/H_2O_2 system. $[MXH_2]$ = 1 mM, $[NaNO_2]$ = 10 mM, [HRP] = 50 μg/ml, and $[H_2O_2]$ = 1 mM. The spectra in A were recorded at 6-min intervals. Reactions were carried out in aerated solutions. Spectrometer settings were microwave power, 5 mW; modulation amplitude, 1.65 G; receiver gain, 5 × 10^3; time constant, 0.125 sec; and scan rate, 4 min/100 G. *Arrow*, directions of changes.

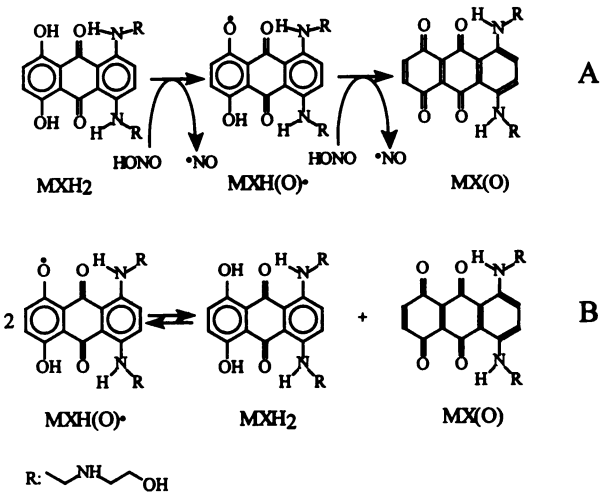

Fig. 8. A, Oxidation of MXH_2 and the MXH_2-derived semiquinone radical $MXH(O)^{\cdot}$ by HNO_2. B, Disproportionation of $MXH(O)^{\cdot}$ radicals generates MXH_2 and a 1,4-quinone form, MX(O), of the drug.

Results of our UV/VIS and EPR measurements suggest that oxidation of MXH_2 by HNO_2 and HRP/H_2O_2 proceeds through the same stages, yielding the oxidized metabolite, MH_2^{2+}, as the major oxidation product, and that other possible processes such as nitrosation or nitration are less important.[4]

The oxidative transformation of MXH_2 to MH_2 is a highly complex multistep process involving irreversible as well as reversible stages, during which one-electron oxidation products, free radicals, and two-electron oxidation products, quinones, and quinone imines can be formed. MXH_2 molecules possess two types of reactive centers that can be attacked by HNO_2: the hydroquinone and the secondary amine (aromatic and alkyl)[5] moieties (20–22). The proposed pathway for the oxidation of MXH_2 by HNO_2 is a two-step process that involves, first, the oxidation of the hydroquinone moiety to a semiquinone radical, $MXH(O)^{\cdot}$, and, second, the oxidation of this radical by another HNO_2 molecule to MX(O), a 1,4-quinone form of the compound (eqs. 6 and 7; Fig. 8A). This mechanism is similar to that proposed for the oxidation of hydrobenzoquinone by HNO_2 (21). Alternatively, the $MXH(O)^{\cdot}$ radicals may be disproportionate to MXH_2 and MX(O) (eq. 8; Fig. 8B).

$$MXH_2 + HNO_2 \rightarrow MXH(O)^{\cdot} + {}^{\cdot}NO + H_2O \quad (6)$$

$$MXH^{\cdot} + HNO_2 \rightarrow MX(O) + {}^{\cdot}NO + H_2O \quad (7)$$

$$2\,MXH^{\cdot} \leftrightarrow MXH_2 + MX(O) \quad (8)$$

The MXH_2-derived radical may also react with $^{\cdot}NO$ and $NO_2^{\cdot}$ radicals produced *in situ* to yield nitrosation and nitration products, respectively. The 1,4-quinone MX(O) is a strong

[4] Products of the reaction of MXH_2 with HNO_2 are identical to those produced by the oxidation of the drug by HRP/H_2O_2 only in the very early stages of the reaction. Mass spectra of samples in which MXH_2 reacted with HNO_2 for 15 min showed an ion with m/z = 470, suggesting the formation of a nitrosated product, presumably MH_2^{2+}—N═O. It is known that in the presence of HNO_2, secondary amines undergo nitrosation to *N*-nitrosoamines.

[5] Ametantrone, a MXH_2 analog that lacks the two OH groups in ring A (Fig. 1), also reacted with HNO_2 (not shown).

electrophile and may react with exogenous electron donors, such as ascorbate or thiols (11–13), but in their absence, it undergoes intramolecular nucleophilic addition to form the cyclized product MH_2 (12, 13). This may occur through the intermediacy of the 5,8-diiminoquinone resonance form MX(N), in which the cyclization process is promoted by an electron-deficient C7 atom (Fig. 9) (12).

It is known that oxidation of MH_2 can also produce free radicals (12). Therefore, the observed EPR signal (Fig. 7) may contain radicals derived from both MXH_2 and MH_2. The MXH_2-derived radicals will dominate during the early stages of drug oxidation, in which MXH_2 either is the only substrate or is present in large excess, but as the reaction progresses and MH_2 accumulates, radicals from the latter compound will become dominant. Thus, depending on the particular reaction conditions as determined by the ratio of [MXH_2] to [oxidant], pH, and aeration, oxidation of MXH_2 may give rise to a mixture of radicals with a varying proportion of semiquinone radicals derived from MXH_2 and MH_2 species. In a situation in which [oxidant] $\gg$ [MXH_2], full conversion to MH_2 or MH_2^{2+} is expected.

The reaction of MXH_2 with HNO_2 is biologically relevant because this acid may be present *in vivo*. HNO_2 is cytotoxic and carcinogenic (30, 31). It causes mutations through deamination of DNA bases (32), oxidizes phenols and hydroquinones (20, 21), and causes nitrosation of secondary amines (22). The possible sources of HNO_2 *in vivo* are nitrite from the diet or that produced *in situ* by cells from $^{\cdot}NO$ (19) and oxygen (eqs. 5–3). Recently, it was suggested that $^{\cdot}NO$ may exert protumor and antitumor activities depending on its local concentration (33). It is known that the cytotoxic action of $^{\cdot}NO$ can be enhanced by the presence of oxygen or superoxide through the formation of more reactive species, such as $NO_2^{\cdot}$, HNO_2, and peroxynitrite ($ONOO^-$). These reactive nitrogen species are involved in the tumoricidal and antibacterial action of macrophages (18, 19, 34), but they also may be harmful to host tissues.

Our study shows that MXH_2 reacts with HNO_2 and perhaps with $^{\cdot}NO$ and $^{\cdot}NO_2$ radicals and suggests a possible biological role for the drug as a scavenger of these highly reactive nitrogen species. Thus, MXH_2, which is administered intravenously, may react directly with the nitrogen species produced by blood components. It is likely that this property may be responsible, at least in part, for the biological activity of the drug *in vivo*. However, further studies are needed to establish whether these reactions are pertinent to the anticancer activity of the drug. The recent discovery of nitric oxide synthase activity in breast cancer cells (35) and the presence in these cells of acidic vesicles (pH = <4) (36) indicate that all conditions that are necessary for the formation of HNO_2 are present in this tumor tissue. These observations are in line with the supposed mechanisms of the biological and, possibly, anticancer action of MXH_2.

In conclusion, MXH_2 undergoes oxidation by nitrite ions in an acid-catalyzed process to give MH_2, a product that is identical to that generated by oxidation of MXH_2 by HRP/H_2O_2. HNO_2 has been identified as the most important oxidizing species, but reaction of the drug with $^{\cdot}NO$ and $NO_2^{\cdot}$ radicals has not been excluded. Because HNO_2 and the $^{\cdot}NO$ and $^{\cdot}NO_2$ radicals can be produced *in vivo* in the acidic environment of tumor cells, our results suggest a new and potentially important role for MXH_2 as a scavenger of these reactive nitrogen species.

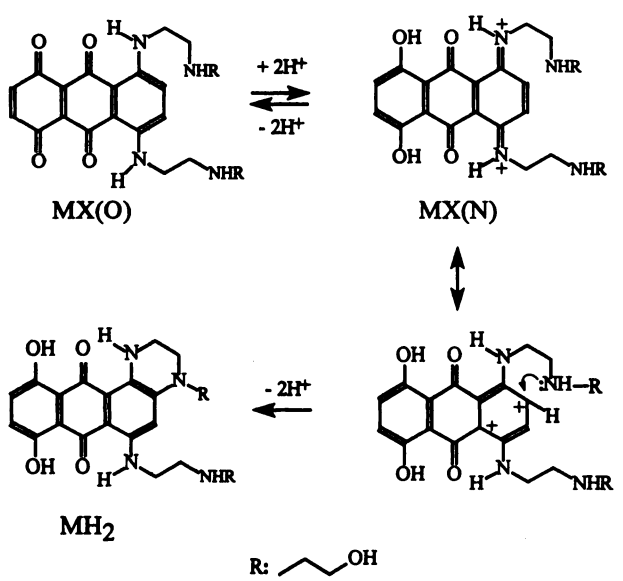

Fig. 9. Equilibrium between the 1,4-quinone and 5,8-diiminoquinone forms of the oxidized MXH_2 and the possible mechanism of the formation of the cyclized product, MH_2.

Acknowledgments

We thank Dr. Kenneth Tomer (Laboratory of Molecular Biophysics, National Institute of Environmental Health Sciences, Research Triangle Park, NC) for providing the mass spectra data.

References

1. Smith, I. E. Mitoxantrone (novantrone): a review of experimental and early clinical studies. *Cancer Treat. Rev.* **10**:103–115 (1983).
2. Faulds, D., J. A. Balfour, P. Chrisp, and H. D. Langtry. Mitoxantrone. A review of its pharmacodynamic and pharmaceutic properties, and therapeutic potential in the chemotherapy of cancer. *Drugs* **41**:400–449 (1991).
3. Zee-Cheng, R. K. Y., and C. C. Cheng. Antineoplastic agents: Structure-activity relationship study of bis(substituted aminoalkylamino)-anthraquinones. *J. Med. Chem.* **21**:291–294 (1978).
4. Arnaiz, S. L., and S. Llesuy. Oxidative stress in mouse heart by antitumoral drugs: a comparative study of doxorubicin and mitoxantrone. *Toxicology* **77**:31–38 (1993).
5. Durr, F. E. Biochemical pharmacology and tumor biology of mitoxantrone and ametantrone, in *Anthracycline And Anthracenedione-Based Anticancer Agents* (J. W. Lown, ed.). Elsevier, New York, 163–200 (1988).
6. Lown, W. J., A. R. Morgan, S.-F. Yen, Y.-H. Wang, and W. D. Wilson. Characteristics of the binding of the anticancer agents mitoxantrone and ametantrone and related structures to deoxyribonucleic acids. *Biochemistry* **24**:4028–4035 (1985).
7. Safa, A. R., N. Chegini, and T. Tseng. Influence of mitoxantrone on nucleic acid synthesis on the T-47D breast tumor cell line. *J. Cell. Biochem.* **22**:111–120 (1983).
8. Kharasch, E. D., and R. F. Novak. Bis(alkylamino)anthracenedione antineoplastic activation by NADPH-cytochrome P-450 reductase and NADPH-dehydrogenase: diminished activity relative anthracyclines. *Arch. Biochem. Biophys.* **224**:682–694 (1983).
9. Fisher, G. R., J. R. Brown, and L. H. Patterson. Redox cycling in MCF-7 human breast cancer cells by antitumor agents based on mitoxantrone. *Free Rad. Res. Commun.* **7**:3–6 (1989).
10. Wolf, C. R., J. S. Macpherson, and J. F. Smyth. Evidence for the metabolism of mitoxantrone by microsomal glutathione transferases and 3-methylcholantrene-inducible glucunorysyl transferases. *Biochem. Pharmacol.* **35**:1577–1581 (1986).
11. Reszka, K., P. Kolodziejczyk, and J. W. Lown. Horseradish peroxidase-catalyzed oxidation of mitoxantrone: spectrophotometric and electron paramagnetic resonance studies. *J. Free Rad. Biol. Med.* **2**:25–32 (1986).
12. Kolodziejczyk, P., K. Reszka, and J. W. Lown. Enzymatic oxidative activation and transformation of the antitumor agent mitoxantrone. *Free Rad. Biol. Med.* **5**:13–25 (1988).
13. Mewes, K., J. Blanz, G. Ehninger, R. Gebhardt, and K.-P. Zeller. Cytochrome P-450-induced cytotoxicity of mitoxantrone by formation of electrophilic intermediates. *Cancer Res.* **53**:5135–5142 (1993).

14. Panousis, C., A. J. Kettle, and D. R. Phillips. Oxidative metabolism of mitoxantrone by the human neutrophil enzyme myeloperoxidase. *Biochem. Pharmacol.* **48**:2223–2230 (1994).
15. Jahde, E., K.-H. Glusenkamp, and M. F. Rajewsky. Protection of cultured malignant cells from mitoxantrone cytotoxicity by low extracellular pH: a possible mechanism for chemoresistance *in vitro*. *Eur. J. Cancer* **26**:101–106 (1990).
16. Bhatnagar, V., S. Anjaiah, N. Puri, B. N. A. Darshanam, and A. Ramaiah. pH of melanosomes of B16 murine melanoma is acidic: its physiological importance in the regulation of melanin biosynthesis. *Arch. Biochem. Biophys.* **307**:183–192 (1993).
17. Ebbing, D. D. *General Chemistry*. 3rd ed. Houghton-Mifflin, Boston (1990).
18. Hibbs, J. B., Jr., R. R. Taintor, and Z. Vavrin. Macrophage cytotoxicity: role for L-arginine deiminase and imino nitrogen oxidation to nitrite. *Science (Washington D. C.)* **235**:473–476 (1987).
19. McCall, T. B., N. K. Boughton-Smith, R. M. Palmer, B. J. Whittle, and S. Moncada. Synthesis of nitric oxide from L-arginine by neutrophils: release and interaction with superoxide anion. *Biochem. J.* **261**:293–296 (1989).
20. Beake, B. D., J. Constantine, and R. B. Moodie. The kinetics and mechanism of reaction of nitrous acid with 4-substituted phenols in aqueous acid solution. *J. Chem. Soc. Perkin Trans. II* **(10)**:1653–1654 (1992).
21. Beake, B. D., R. B. Moodie, and J. P. B. Sandall. The kinetics and mechanism of oxidation of hydroquinone and chlorohydroquinone in the presence of nitrous acid in aqueous solution. *J. Chem. Soc. Perkin Trans. II* **(5)**:957–960 (1994).
22. Kato, T., N. Tadokoro, M. Tsutsui, and K. Kikugawa. Transformation of arylamines into direct-acting mutagens by reaction with nitrite. *Mutat. Res.* **249**:243–254 (1991).
23. Kapuscinski, J., Z. Darzynkiewicz, F. Traganos, and M. R. Melamed. Interactions of a new antitumor agent, 1,4-dihydroxy-5,8-bis[[2-[2-hydroxyethyl)amino]-ethyl]amino]-9,10-anthracenedione, with nucleic acids. *Biochem. Pharmacol.* **30**:231–240 (1981).
24. Kapuscinski, J., and Z. Darzynkiewicz. Interactions of antitumor agents Ametantrone and mitoxantrone (Novantrone) with double-stranded DNA. *Biochem. Pharmacol.* **34**:4203–4213 (1985).
25. Prutz, W. A. Tyrosine oxidation by $NO_2^{\cdot}$ in aqueous solution. *Z. Naturforsch.* **39C**:725–727 (1984).
26. Prutz, W. A., H. Monig, J. Butler, and E. J. Land. Reactions of nitrogen dioxide in aqueous model systems: oxidation of tyrosine units in peptides and proteins. *Arch. Biochem. Biophys.* **243**:125–134 (1985).
27. Huie, R. E., and P. Neta. Kinetics of one-electron transfer reactions involving ClO_4 and NO_2. *J. Phys. Chem.* **90**:1193–1198 (1986).
28. Janzen, E. G., A. L. Wilcox, and V. Manoharan. Reactions of nitric oxide with phenolic antioxidants and phenoxyl radicals. *J. Org. Chem.* **58**:3597–3599 (1993).
29. Wilcox, A. L., and E. G. Janzen. Nitric oxide reactions with antioxidants in model systems: sterically hindered phenols and α-tocopherol in sodium dodecyl sulfate (SDS) micelles. *J. Chem. Soc. Chem. Commun.* **(18)**:1377–1379 (1993).
30. Zimmermann, F. K. Genetic effects of nitrous acid. *Mutat. Res.* **39**:127–148 (1977).
31. Routledge, M. N., F. J. Mirsky, D. A. Wink, L. K. Keefer, and A. Dipple. Nitrite induced mutations in a forward mutation assay: influence of nitrite concentration and pH. *Mutat. Res.* **322**:341–346 (1994).
32. Coulondre, C., J. H. Miller, P. J. Farabaugh, and W. Gilbert. Molecular basis of base substitution hotspots in *Escherichia coli*. *Nature (Lond.)* **274**:775–780 (1978).
33. Jenkins, D. C., I. G. Charles, L. L. Thomsen, D. W. Moss, L. S. Holmes, S. A. Baylis, P. Rhodes, K. Westmore, P. C. Emson, and S. Moncada. Roles of nitric oxide in tumor growth. *Proc. Natl. Acad. Sci. USA* **92**:4392–4396 (1995).
34. Castellani, A. G., and C. F. Niven, Jr. Factors affecting the bacteriostatic action of sodium nitrite. *Appl. Microbiol.* **3**:154–159 (1955).
35. Thomsen, L. L., D. W. Miles, L. Happerfiled, L. G. Bobrow, R. G. Knowles, and S. Moncada. Nitric oxide synthase activity in human breast cancer. *Br. J. Cancer* **72**:41–44 (1995).
36. Montcourrier, P., P. H. Mangeat, C. Valembois, G. Salazar, A. Sahuquet, C. Duperray, and H. Rochefort. Characterization of very acidic phagosomes in breast cancer cells and association with invasion. *J. Cell. Sci.* **107**:2381–2391 (1994).

Send reprint requests to: Dr. Krzysztof J. Reszka, Laboratory of Molecular Biophysics, NIEHS, NIH, P.O. Box 12233, Research Triangle Park, NC 27709. E-mail: reszka@niehs.nih.gov